Supplementary Information (SI) for Journal of Materials Chemistry A.

Ultra-thin anodes with controlled thickness modified by in situ Li_3N for high-energy-density lithium metal batteries

Hong Chen[a], Weimin Chen[a,*], Du Tian[a], Lanying Chen[a], Xianchao Zhao[a], Dou Mao[a], Yue Shen[b], Faquan Yu[a,*]

[a] H. Chen, D. Tian, L. Chen, X. Zhao, D. Mao, Prof. W. Chen, Prof. F. Yu

Key Laboratory for Green Chemical Process of Ministry of Education, Hubei Key Laboratory for Novel Reactor and Green Chemistry Technology, Hubei Engineering Research Center for Advanced Fine Chemicals, School of Chemical Engineering and Pharmacy, Wuhan Institute of Technology, Wuhan 430205, China.

E-mail: wmchen@wit.edu.cn; fyu@wit.edu.cn

[b] State Key Laboratory of Materials Processing and Die & Mould Technology, School of Materials Science and Engineering, Huazhong University of Science and Technology, Wuhan 430074, China.

Experimental Section

1.1Synthesis of NCF/rGO Film

First, 80 mL of 4 mg mL^{-1} graphene oxide (GO) solution was measured, 20 μL of pyrrole and 0.08 g of cetyltrimethylammonium bromide (CTAB) were added, and stirred for 30 min at 0-5°C. Then 0.068 g of ammonium persulfate (APS) was dissolved in 1 mL of water and added dropwise. After stirring for 30 minutes, 20 mL of the mixed solution was taken and filtered through a Brinell filter and lyophilised to form PPy/GO films; finally, the film material was carbonised under argon protection by heating to 250°C for 30 min and then to 600°C for 4 h to obtain the NCF/rGO films.

The rGO films were prepared using the same method: 20 mL of a 4 mg mL^{-1} solution of graphene oxide (GO) was measured and pumped through a Brinell filter, followed by lyophilisation to form a film; finally, the rGO films were obtained by carbonising the film material again.

1.2 Synthesis of NCF/rGO/Li_3N Film

Lithium metal is heated to 350 °C to form a molten state in an argon glove box with an O_2 and H_2O content of less than 0.01 ppm. One side of the above NCF/rGO film was then contacted with the molten lithium to form Li_3N. After cooling to room temperature, the NCF/rGO/Li_3N film was punched into a round electrode of 8 mm. For comparison, rGO/Li electrode was prepared using a similar method.

If not otherwise specified, the films obtained from the above scheme are those

used in electrochemical testing experiments, and the thickness of the electrodes in the experimental and control groups is about 25 μm.

1.3 Characterization

The morphologies and structural features of the resulting electrodes were investigated by field emission scanning electron microscopy (FESEM, Nova 8 NanoSEM450), transmission electron microscopy (JEOL JEM-ARF200f). The material composition was characterised by X-ray diffraction (XRD, Philips, using Cu Ka as the radiation source, $\lambda = 0.15406$ nm, the scanning rate of 5º min^{-1} and scanning angle of 5º~90º). FT-IR spectra were obtained on a JASCO FT/IR4100 spectrometer. Energy dispersive X-ray spectrometry (EDX) and X-ray photoelectron spectroscopy (XPS, AXISULTRADLD) were used to analyse the elemental distribution and content of the samples. TOF-SIMS was conducted using an ION-TOF (Gmhb 5, Münster, Germany) with an Ar-ion beam.

1.4 Electrochemical measurement

The CR2032-type coin cells and pouch cells were fabricated inside an Ar-filled glove box. The thin Li foil (50 μm) obtained from Tianjin Zhongneng Lithium Co, Ltd. The separator is polypropylene membrane (Celgard, 2400 PP). Unless explicitl stated, all cells utilized a 1 M lithium bis (trifluoromethanesulfonyl) imide (LiTFSI) carbonate electrolyte dissolved in a 1:1 mixture of 1,3-dioxolane (DOL) and 1,2-dimethoxyethane (DME) with the addition of 2 wt% $LiNO_3$.

Li||Li symmetric cells were configured with two identical bare Li foils or two

rGO/Li and two NCF/rGO/Li_3N as working and counter electrodes. The polarisation characteristics during lithium plating/stripping at constant current density were evaluated using symmetric cells.

Full cells were assembled to evaluate the feasibility of NCF/rGO/Li_3N anode. To prepare $LiFePO_4$ (LFP) cathode, active materials, carbon black, and polyvinylidene fluoride (PVDF) binder (mass ratio 8:1:1) were dispersed in N-methyl-2-pyrrolidone (NMP) solvent. The slurry was casted on Al foil and dried at 60 °C for 24 h before assembling. The LFP cathode had an isomass loading of 2 mg cm^{-2}. The high-loading LFP (17 mg cm^{-2}) electrodes were purchased. The constant current charge/discharge process was performed on Land CT2001A system with a voltage range of 2.5 – 4.0 V (vs Li^+/Li). The NCM811(4 mAh cm^{-2}) cathode had an isomass loading of 20 mg cm^{-2} with 1.2 M $LiPF_6$ in ethylene carbonate (EC)/ethyl methyl carbonate (EMC) /fluoroethylene carbonate (FEC) as the electrolyte (purchased from Guangdong Canrd New Energy Technology Co. Ltd). The lithium metal||NCM811 battery constant current charge/discharge process voltage range is 3.0 – 4.3 V (for Li^+/Li).

The pouch cells with all other conditions remaining constant as in the case of coin cells. The dimension of the cathode material was 30 mm × 40 mm and the area for anode material was 32 mm × 42 mm, the electrolyte used here was composed of 1.0 M $LiPF_6$ in EC/EMC (v/v=3:7).

Half cells are used to test ACE and nucleation overpotentials with copper foil, rGO film or NCF/rGO film as anode and lithium foil as cathode. Li||Cu coin cells

using copper foil as the cathode and bare lithium, rGO/Li or NCF/rGO/Li_3N electrodes as the anode, Li||Cu coin cells are used to test CE and GITT. The various tests for electrode thickness were conducted by testing the areal capacity using a Li||Cu coin cell with 1.0 V (vs Li^+/Li) for stripping Li.

The cells were tested for galvanostatic charge-discharge using the Land CT2001A systems. EIS, CV, Tafel and Li-ion transfer numbers tests were conducted using the CHI 760E electrochemical workstation. Among them, the frequency range of 100 KHz to 0.01 Hz was used for probing EIS measurements, the CV for full cells were obtained at a scanning rate of 0.1 mV s^{-1} from 2.5 to 4.0 V, the Tafel for symmetric cells were probed at 1 mV s^{-1} from −0.15 to 0.15 V. The exchange current density was calculated based on Tafel equation:

$$\eta = a + b\log(j) \qquad \text{(Equation S1)}$$

where j is the current density, η is the overpotential, a and b are constants.

Li-ion transfer numbers were measured by chronoamperometry with a polarization voltage of 10 mV applied for 4000 s and calculated using the following equation:

$$t_{Li^+} = \frac{I_S(\Delta V - I_0 R_0)}{I_O(\Delta V - I_S R_S)} \qquad \text{(Equation S2)}$$

where ΔV is the polarization voltage, I_0 and I_S are the initial and steady-state currents, and R_0 and R_S are the initial and steady-state interfacial resistances obtained from EIS, respectively. Cyclic voltammetry test was conducted at the voltage from −0.2 to 0.2 V at the scan rate of 0.2 mV s^{-1}.

The energy density E_g of the full cell is calculated according to the following equation：

$$E_g = \frac{vC}{m} \qquad \text{(Equation S3)}$$

where E_g is the full-cell gravimetric (Wh kg^{-1}) energy densities, respectively, v is the average output voltage (3.8 V is assumed), C is the capacity (mAh).

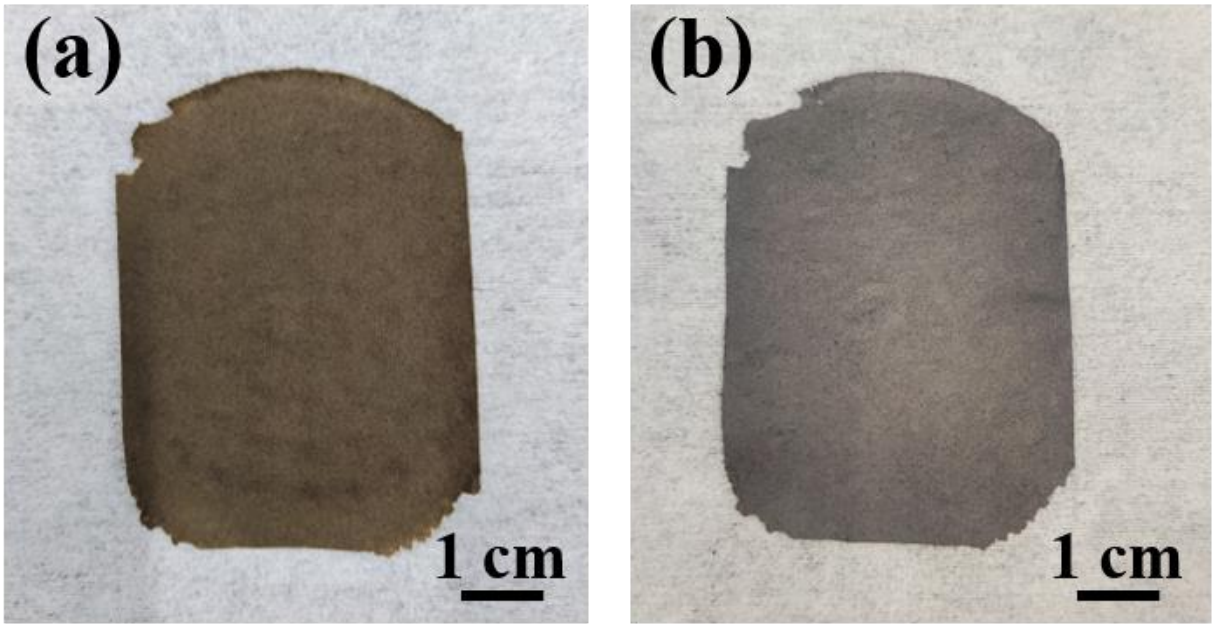

Fig. S1. Physical images of (a) PPy/GO, (b) NCF/rGO.

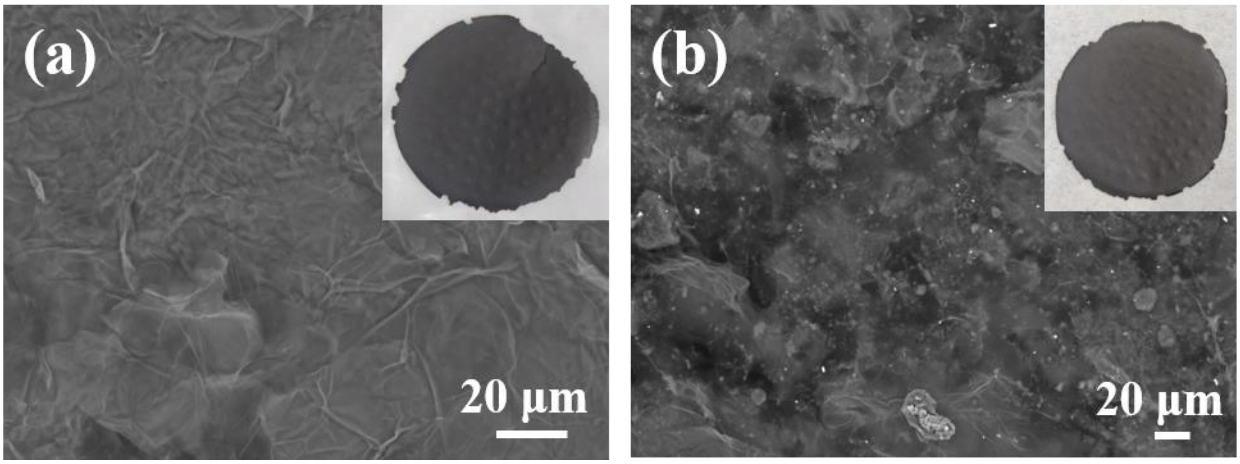

Fig. S2. SEM inages of (a) rGO, (b) NCF/rGO.

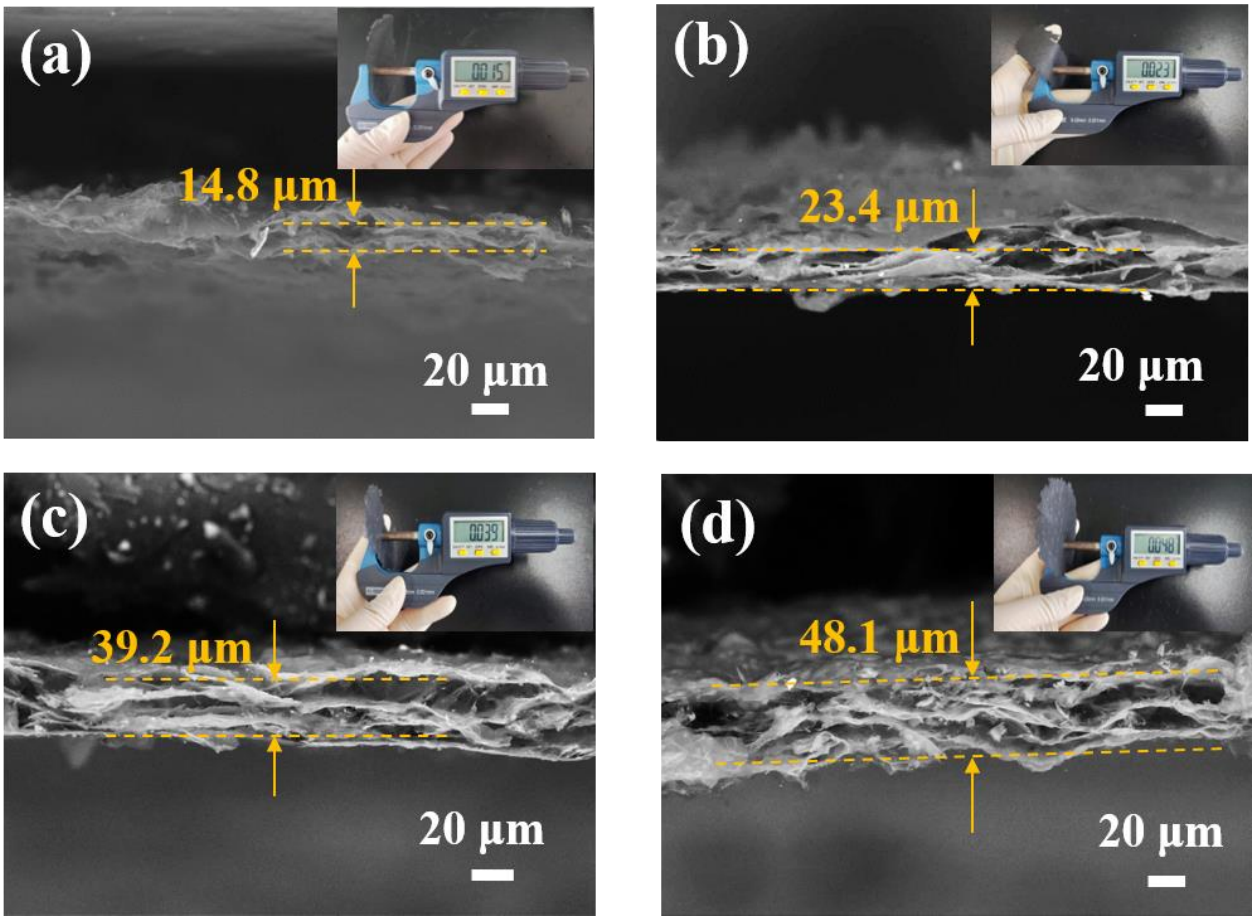

Fig. S3. Cross-sectional SEM of NCF/rGO films of different thicknesses. (Inset: digital photos of NCF/rGO films with different thicknesses) The thickness of the NCF/rGO films can be controlled by varying the volume of the pumped filtration: (a) 10 mL, (b) 20 mL, (c) 30 mL, (d) 40 mL.

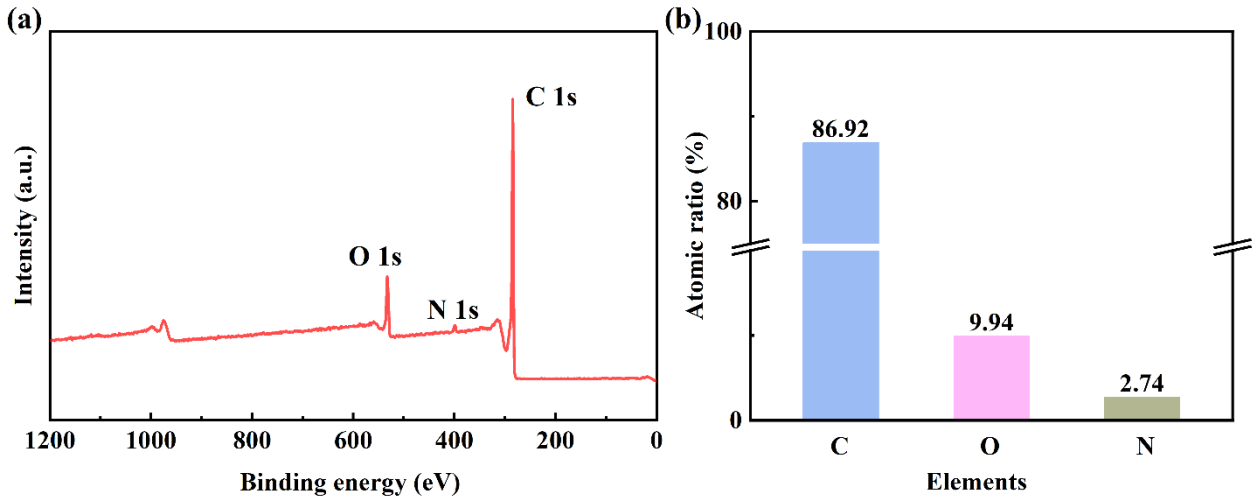

Fig. S4. (a) XPS survey spectrum of NCF/rGO. (b) Ratio of C, N, O elements in the XPS results.

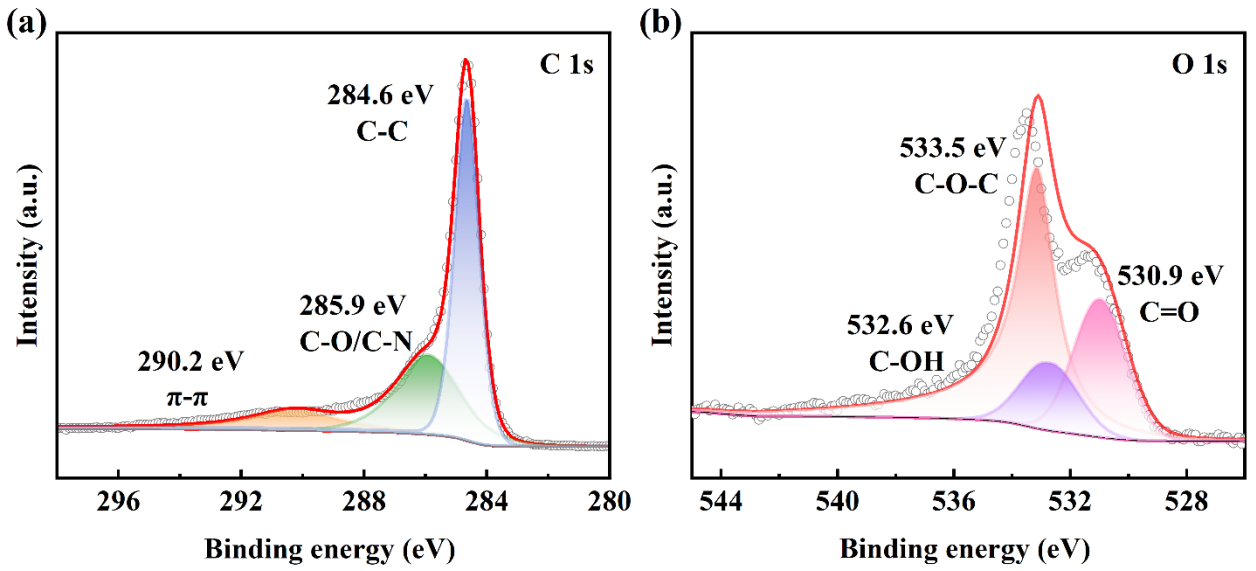

Fig. S5. High-resolution XPS spectra of NCF/rGO for (a) C 1s, (b) O 1s.

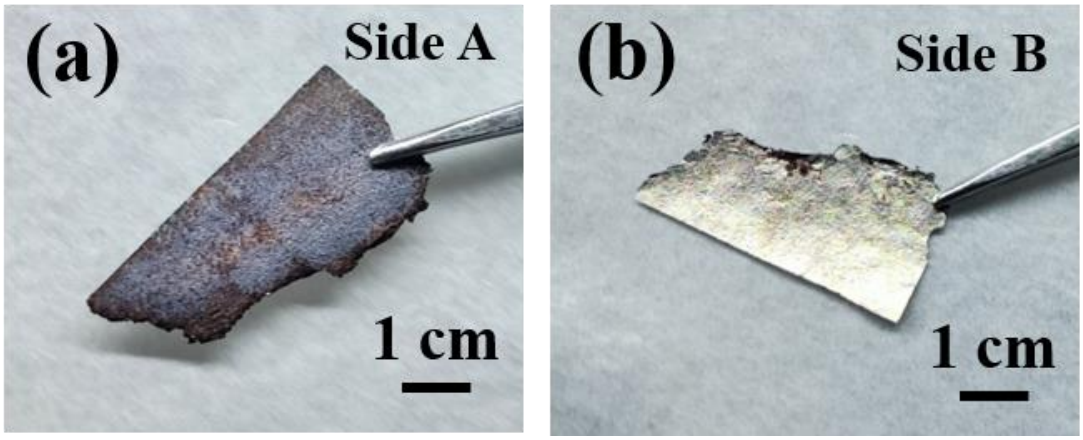

Fig. S6. Physical images of NCF/rGO/Li_3N.

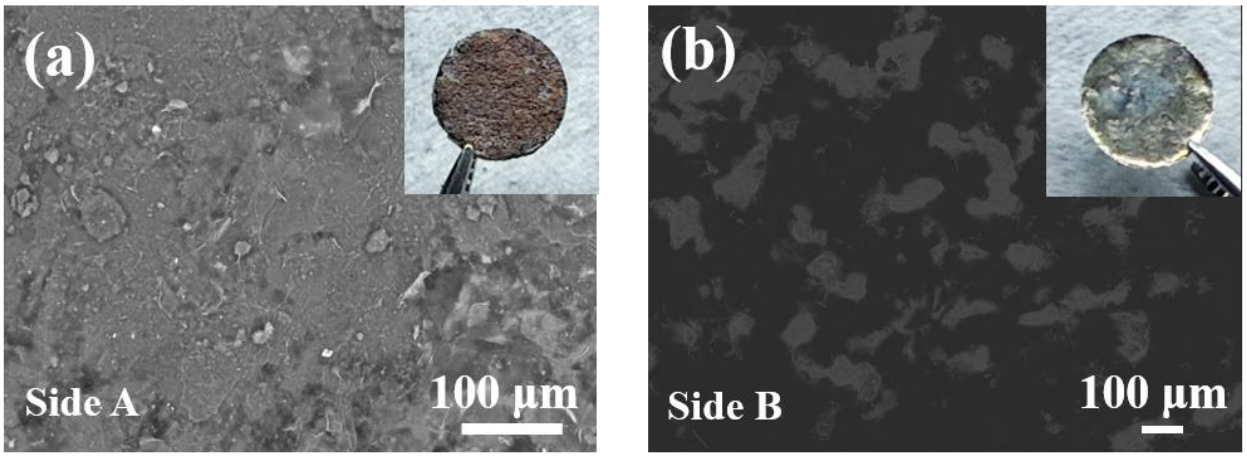

Fig. S7. SEM images of NCF/rGO/Li_3N.

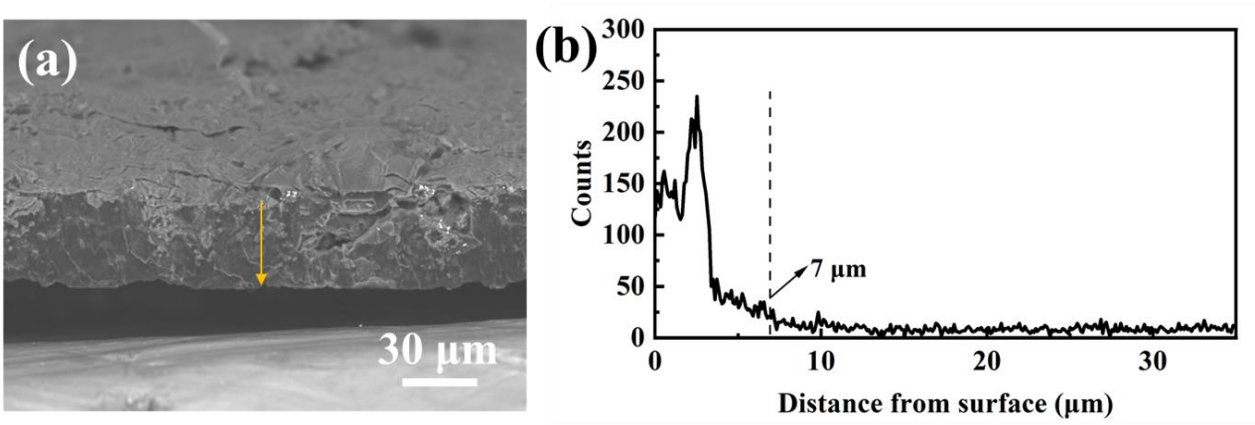

Fig. S8. Cross-section N element distribution of sample NCF/rGO/Li_3N anode line scanning results of energy spectrometer.

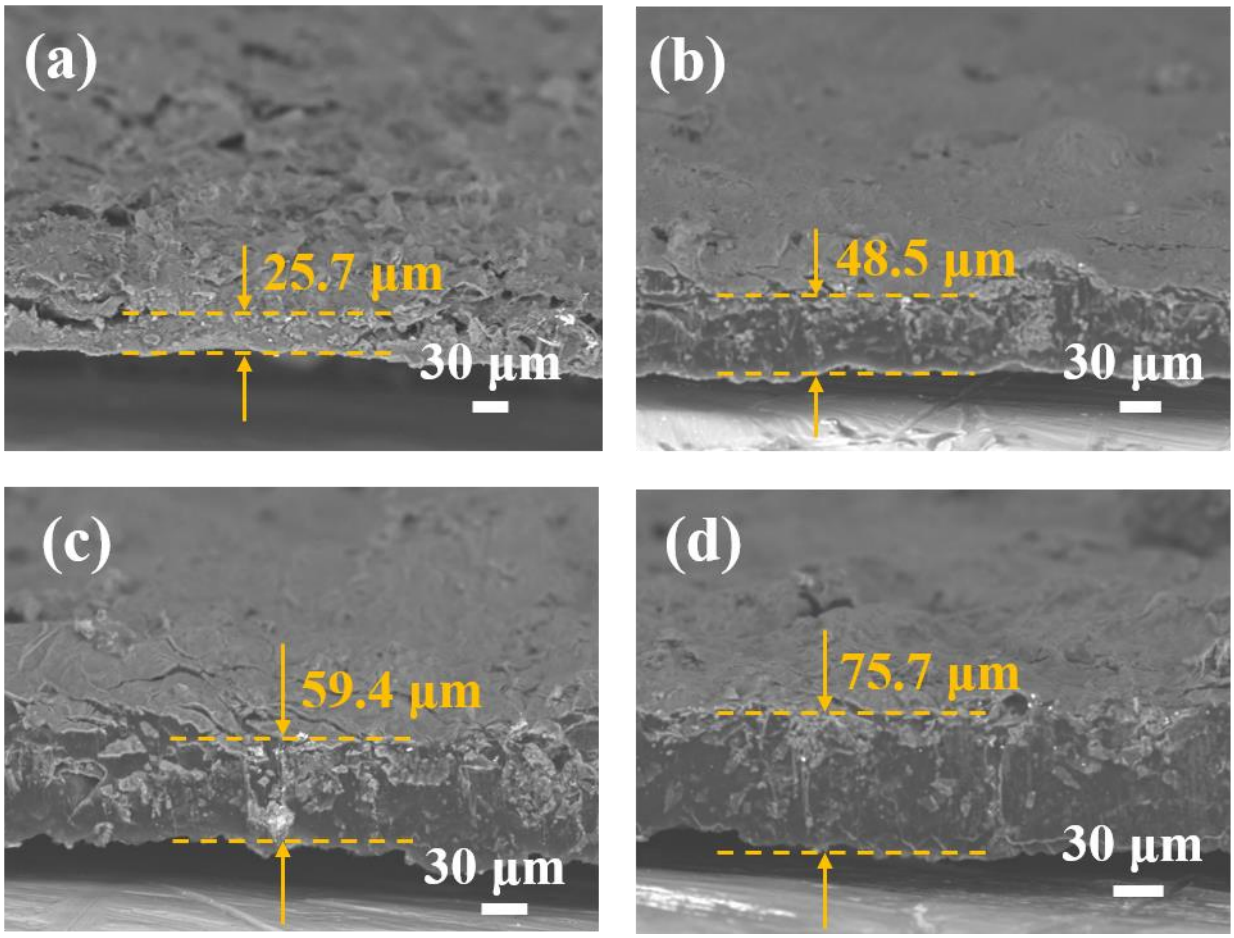

Fig. S9. Cross-sectional SEM of NCF/rGO/Li_3N films of different thicknesses.

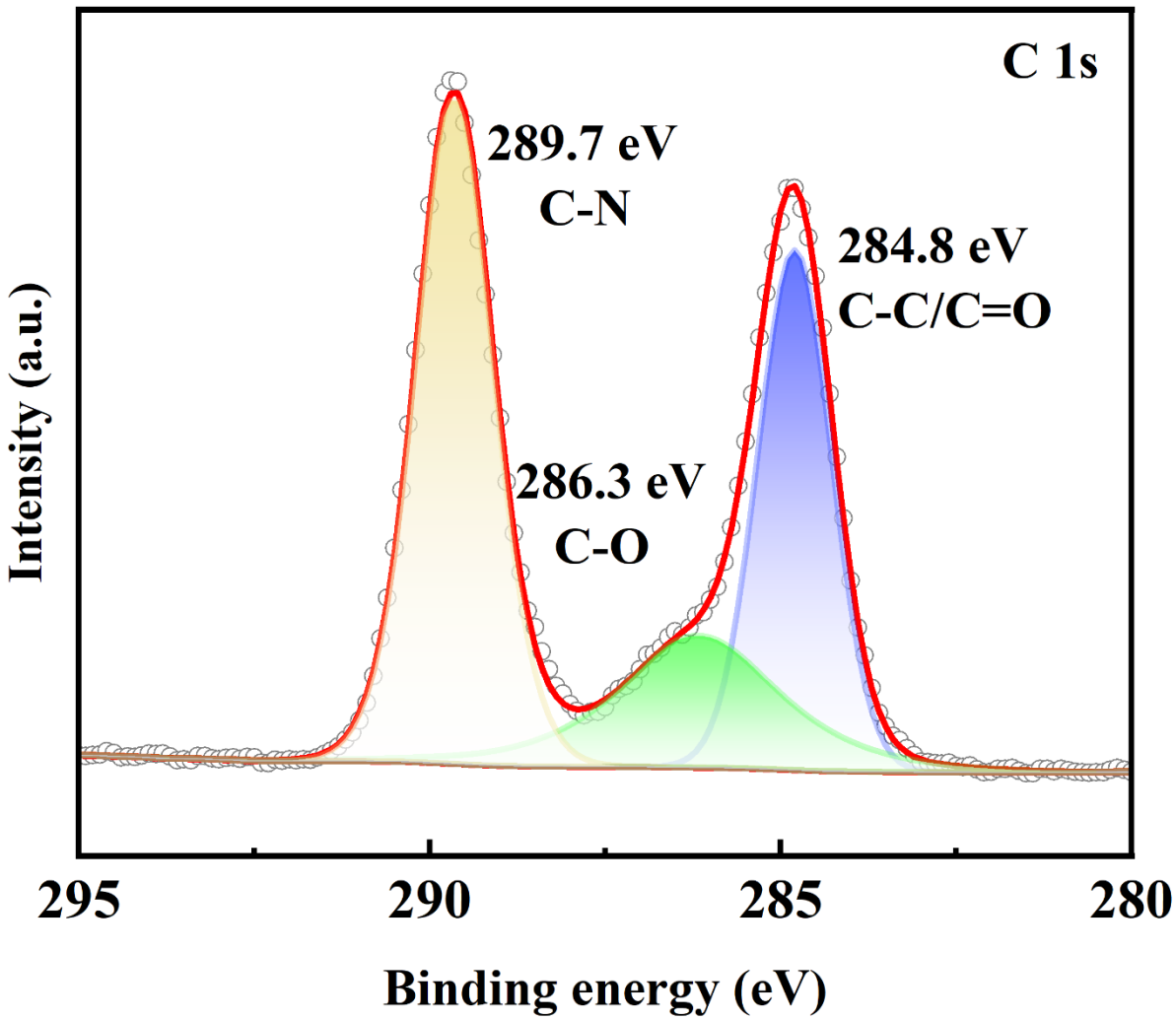

Fig. S10. High-resolution XPS spectra of NCF/rGO/Li_3N for C 1s.

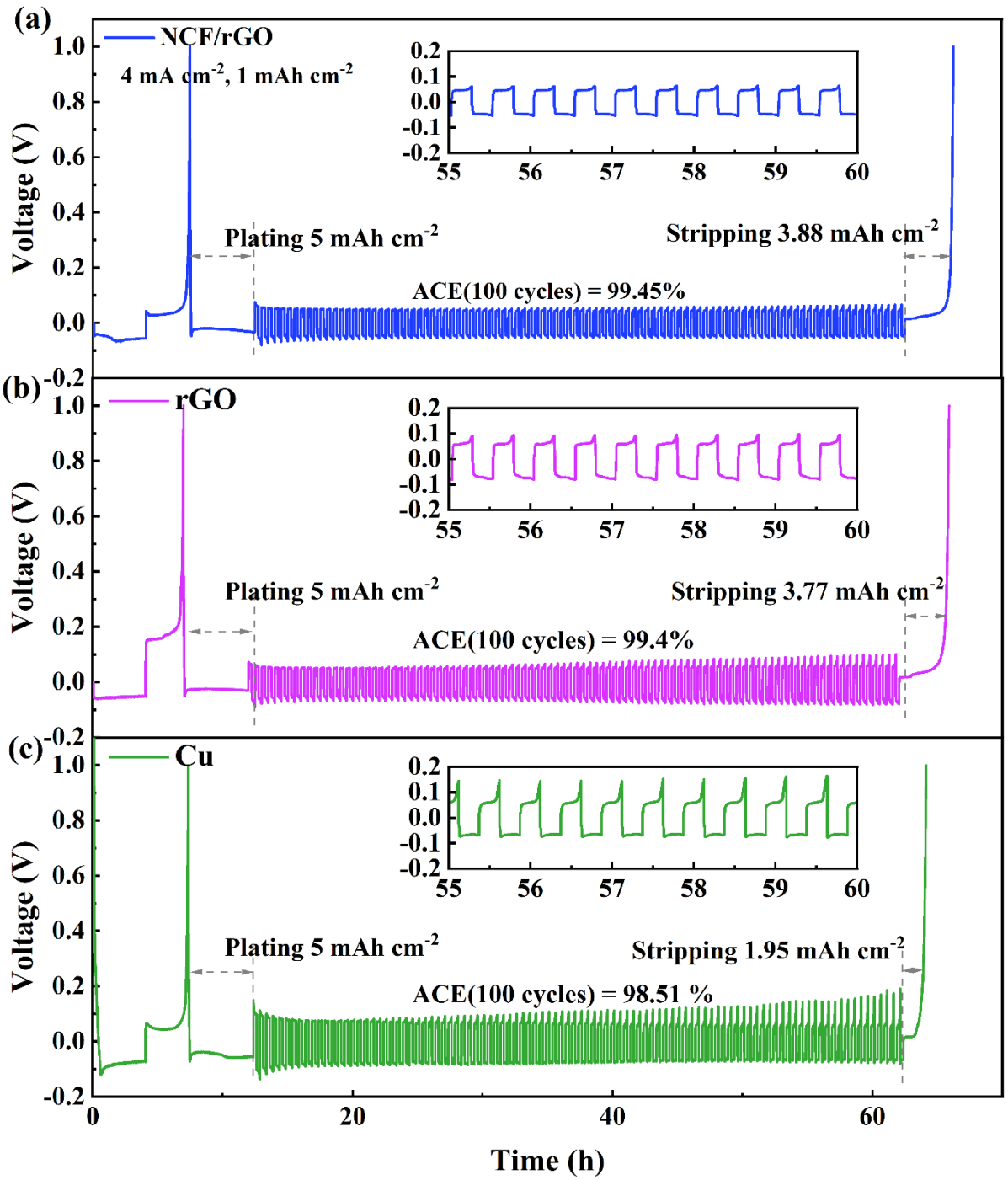

Fig. S11. Average CE of half-cells assembled with (a) Cu, (b) rGO, (c) NCF/rGO at 4 mA cm^{-2} and 1mAh cm^{-2}.

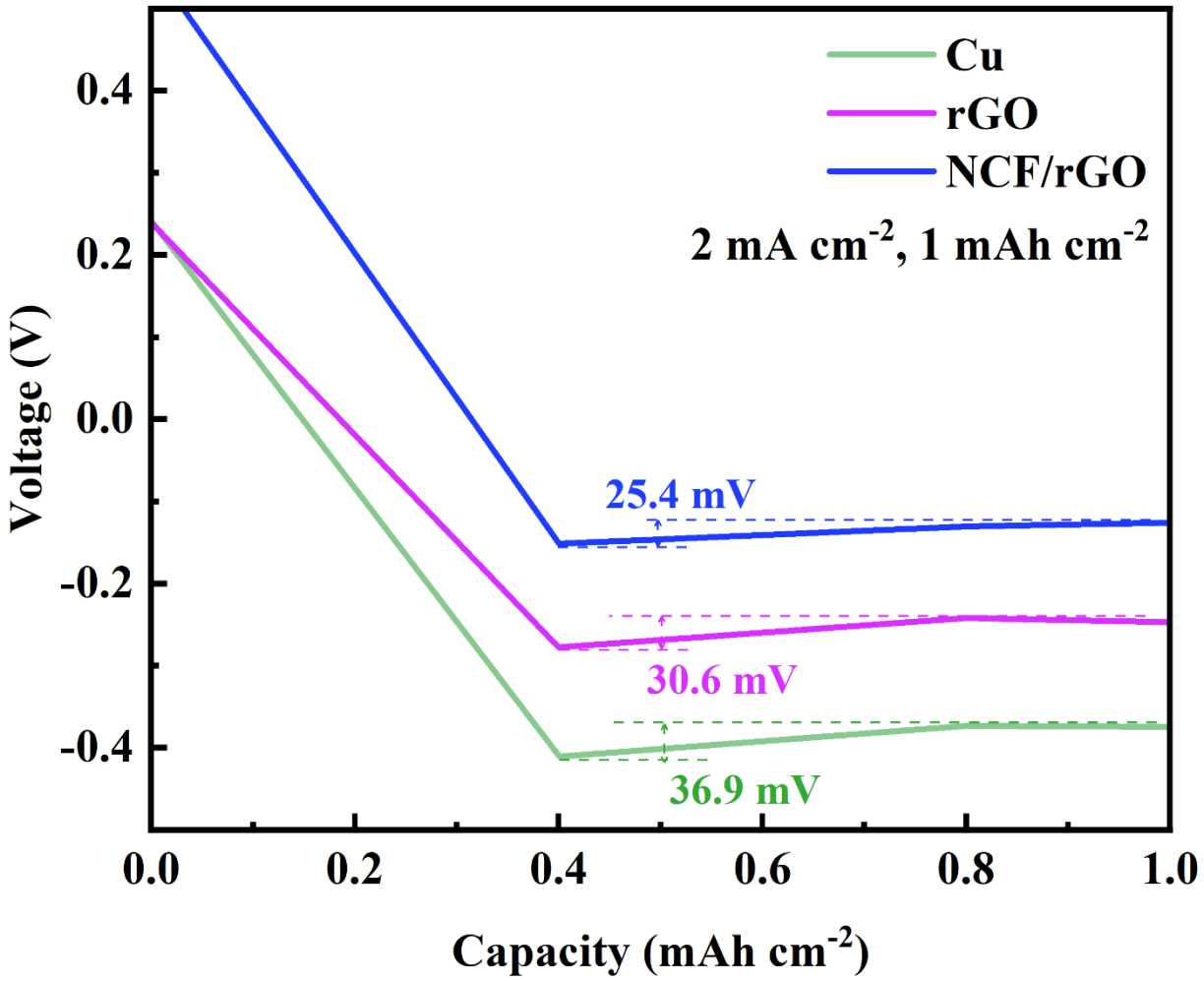

Fig. S12. Nucleation overpotential of half-cells assembled with Cu, rGO and NCF/rGO at 2 mA cm^{-1} and 1 mAh cm^{-2}.

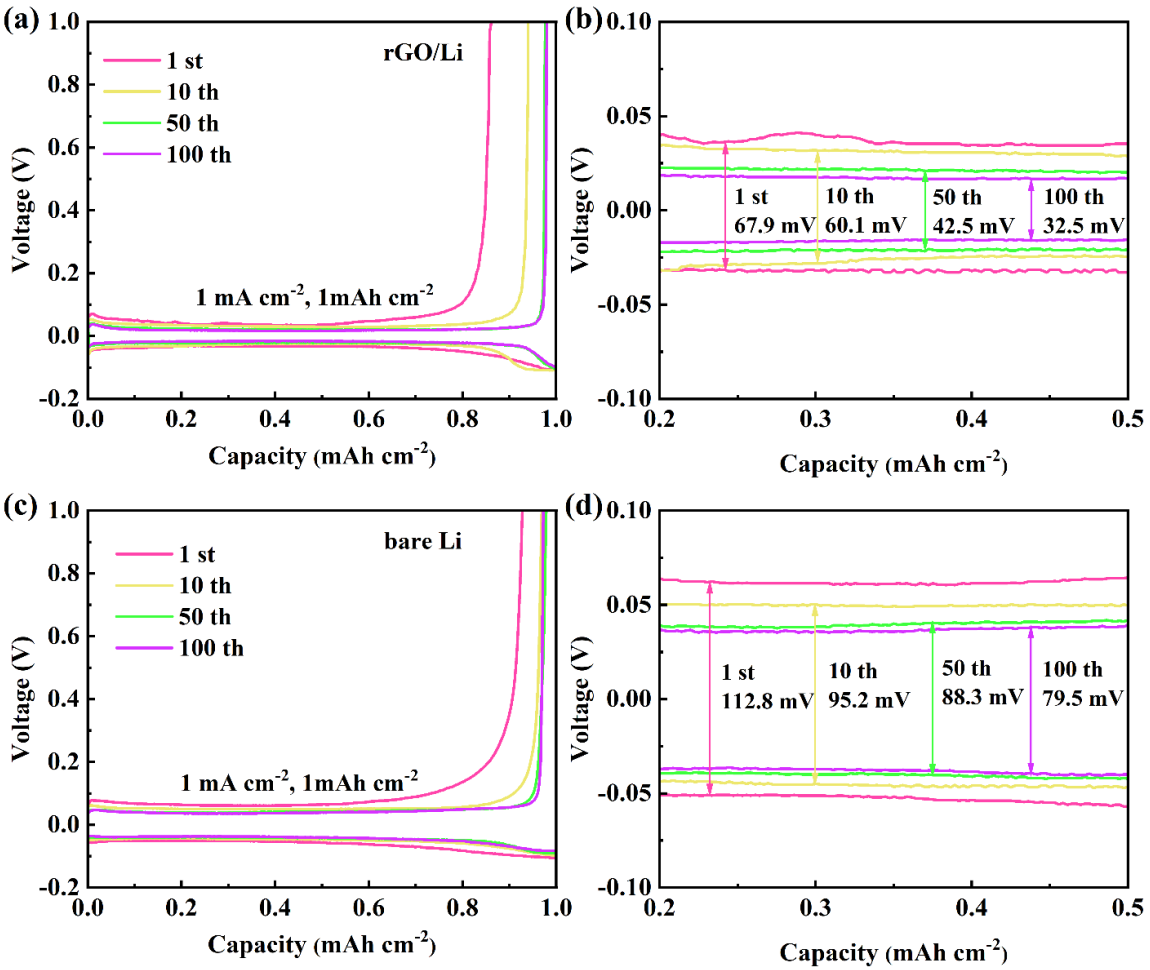

Fig. S13. Voltage profiles in different cycles of the Li plating/stripping process on (a-b) rGO/Li and (c-d) bare Li electrodes at 1 mA cm^{-2} with fixed capacity of 1 mAh cm^{-2}.

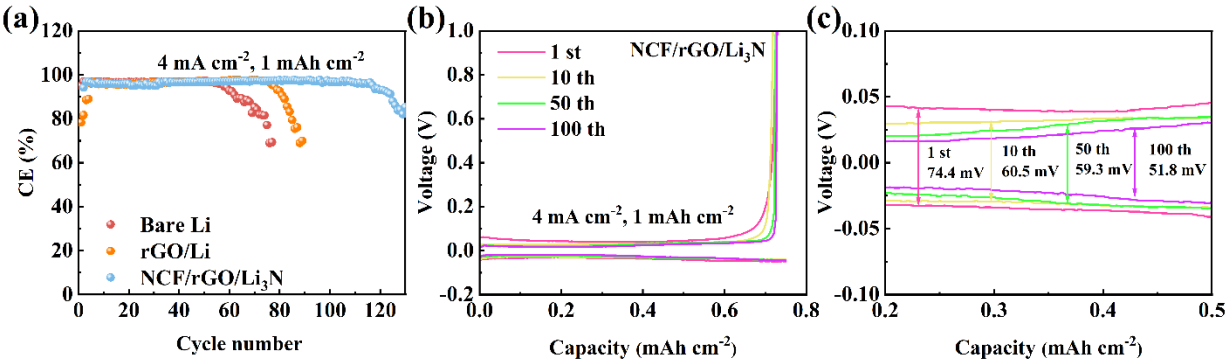

Fig. S14. The Coulombic efficiency for NCF/rGO/Li_3N, rGO/Li and bare Li with the current density of (a) 4 mA cm^{-2} at 1 mAh cm^{-2}. (b-c) Voltage profiles on NCF/rGO/Li_3N electrode.

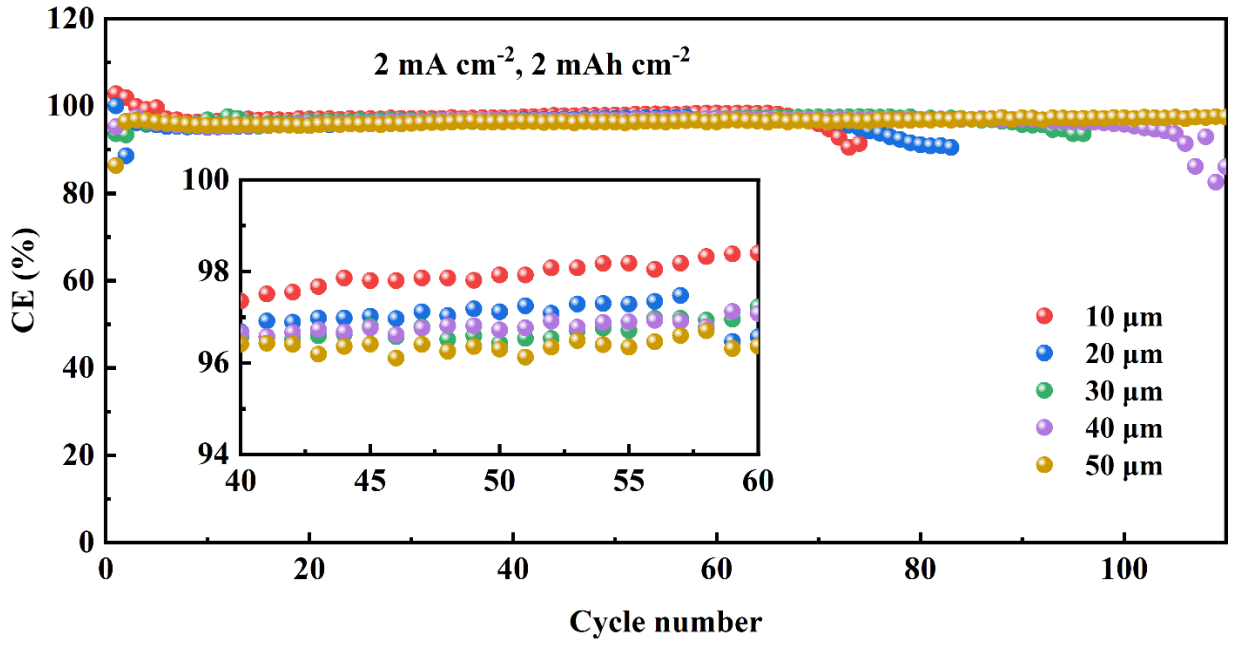

Fig. S15. Coulombic efficiency of NCF/rGO/Li_3N||Cu half-cells with different thicknesses at 2 mA cm^{-2} and 2 mAh cm^{-2}.

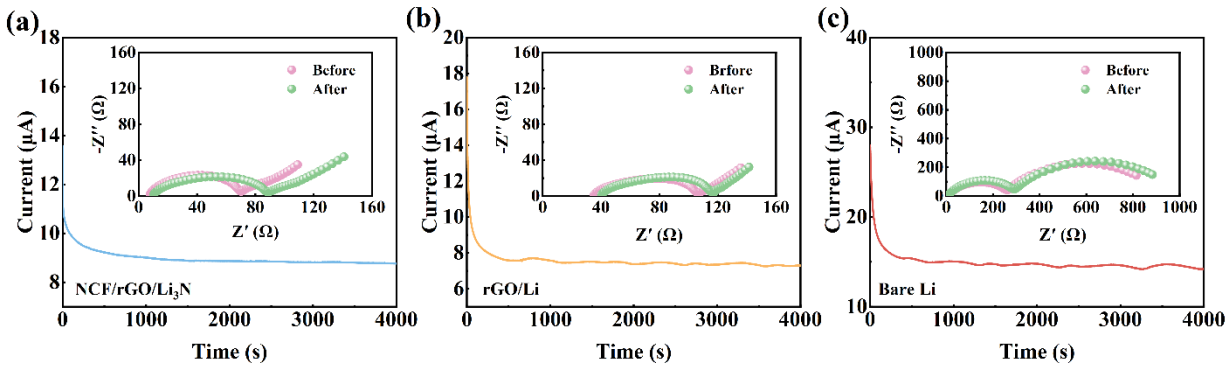

Fig. S16. Chronoamperometry spectra of (a) NCF/rGO/Li_3N, (b) rGO/Li and (c) bare Li symmetric cells at 10 mV polarization voltage and the corresponding EIS curves before and after polarization (inset).

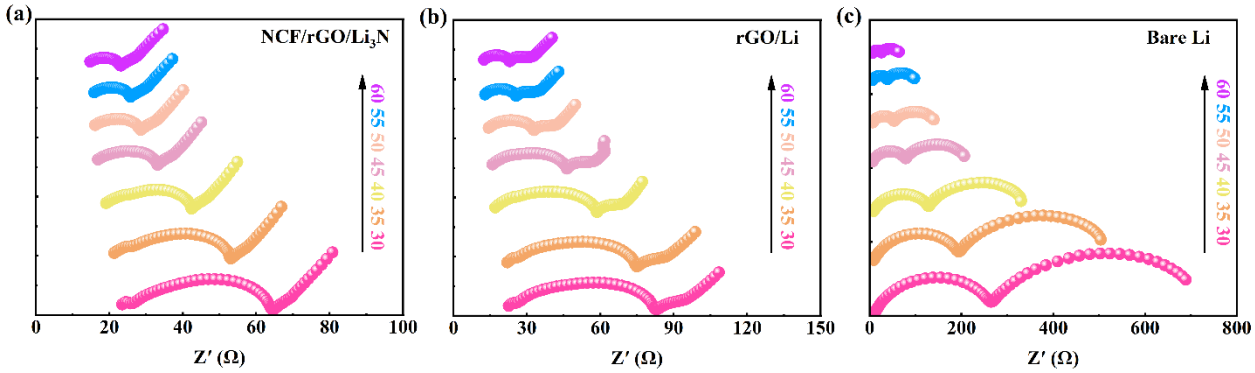

Fig. S17. Temperature-dependent EIS spectra of (a) NCF/rGO/Li_3N, (b) rGO/Li and (c) bare Li symmetric cells; temperatures are marked in corresponding colors.

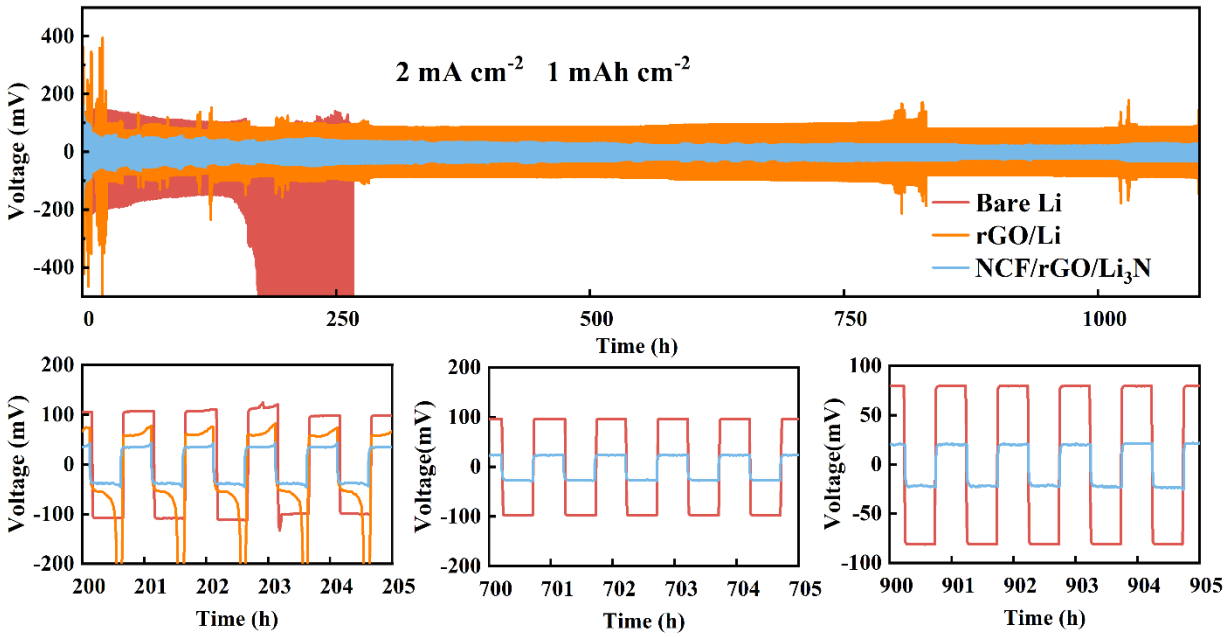

Fig. S18. Voltage-time profiles of the symmetric cells with NCF/rGO/Li_3N, rGO/Li and bare Li electrodes at 2 mA cm^{-2}, 1 mAh cm^{-2}.

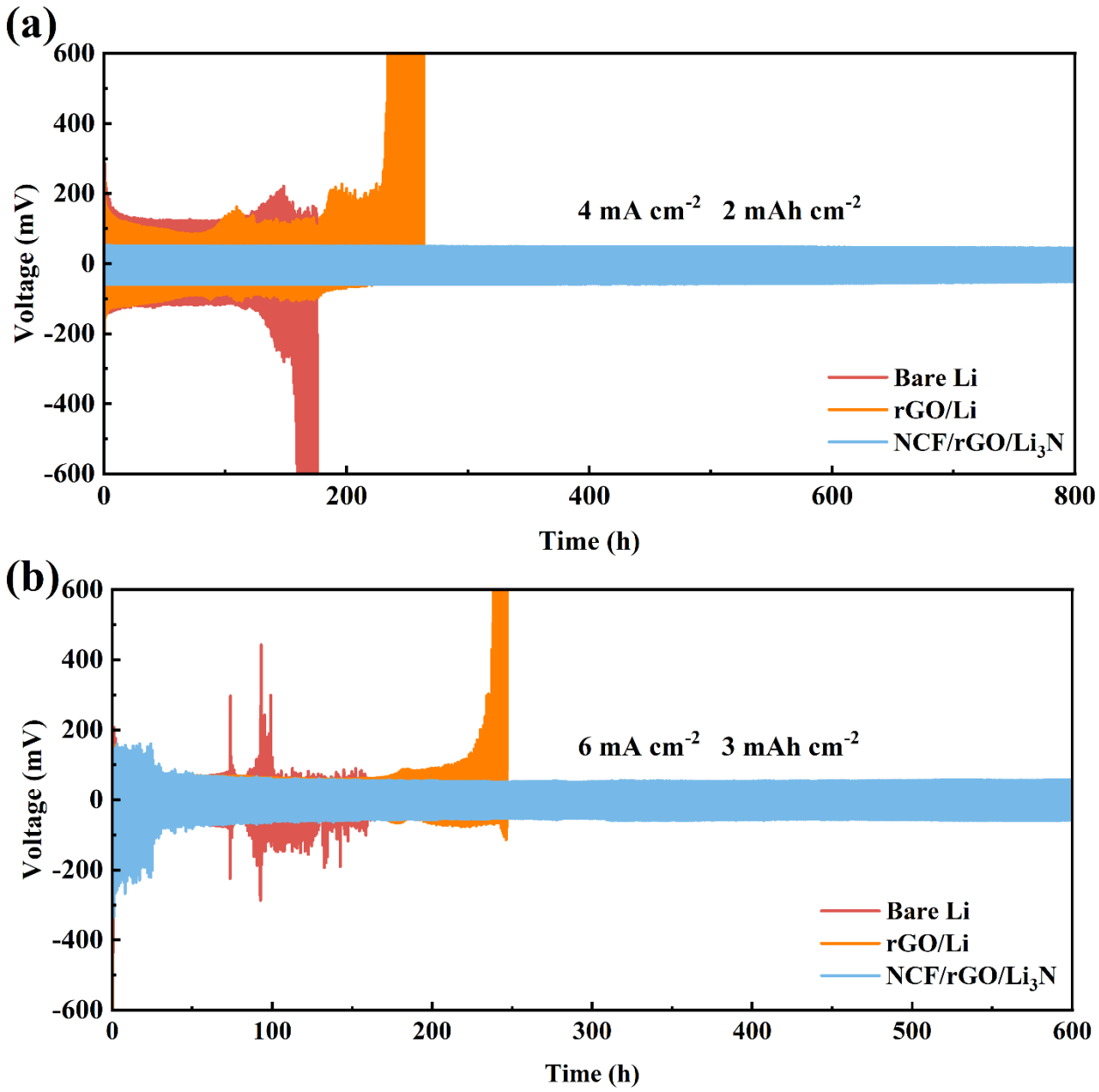

Fig. S19. Voltage-time profiles of the symmetric cells with NCF/rGO/Li_3N, rGO/Li and bare Li electrodes. (a) 4 mA cm^{-2}, 2 mAh cm^{-2} and (b) 6 mA cm^{-2}, 3 mAh cm^{-2}.

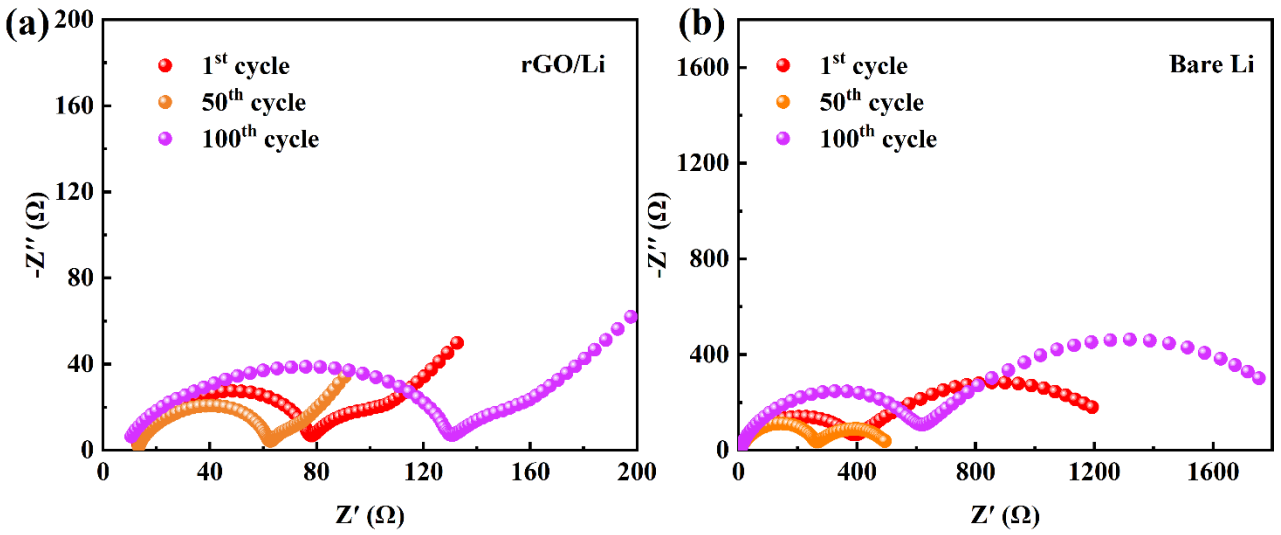

Fig. S20. Nyquist plots of (a) rGO/Li and (b) Bare Li symmetric cells after 1 cycle, after 50 cycles and after 100 cycles at 1 mA cm^{-2}, 0.5 mAh cm^{-2}.

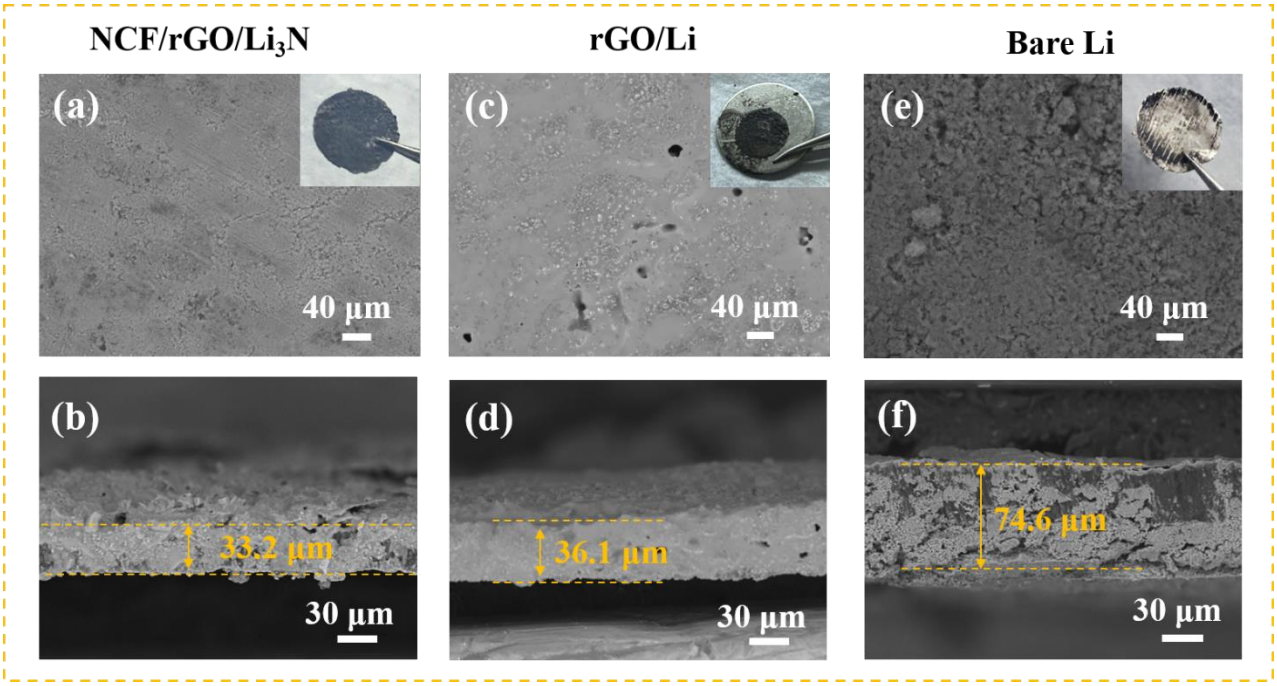

Fig. S21. SEM images of the (a) NCF/rGO/Li_3N, (b) rGO/Li and (c) bare Li electrodes at 1 mA cm^{-2} and 1 mAh cm^{-2} after 100 cycles.

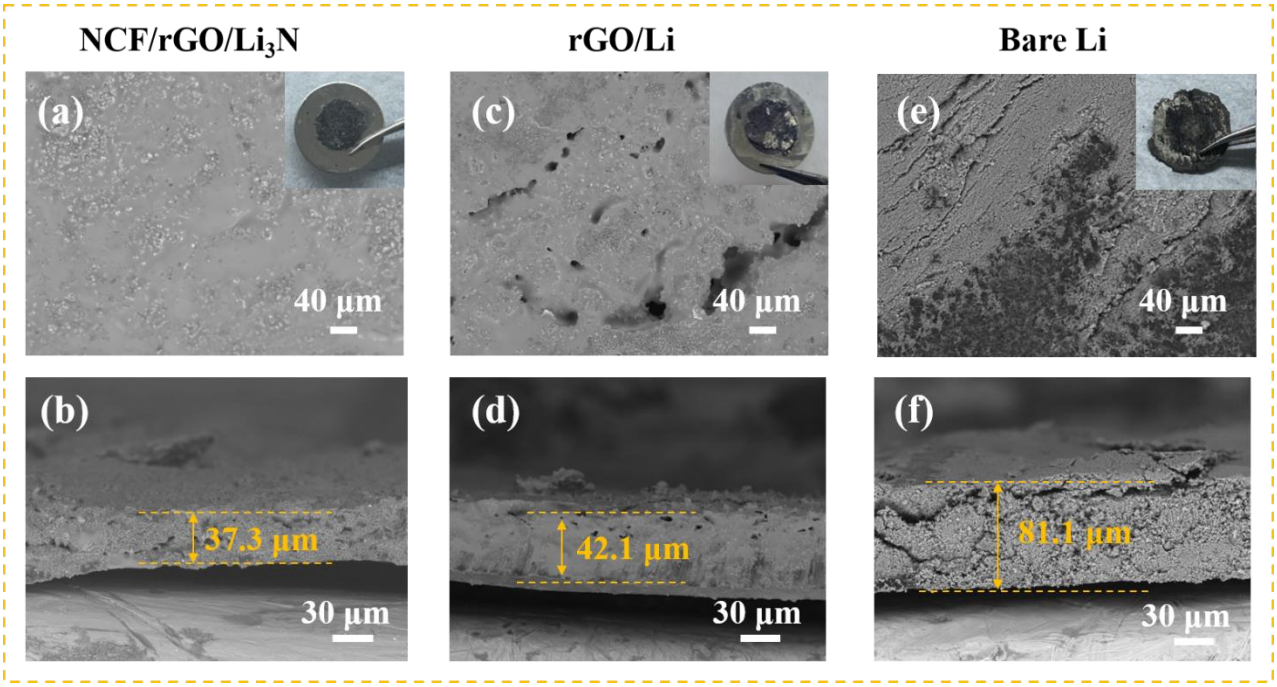

Fig. S22. SEM images of the (a) NCF/rGO/Li_3N, (b) rGO/Li and (c) bare Li electrodes at 2 mA cm^{-2} and 1 mAh cm^{-2} after 100 cycles.

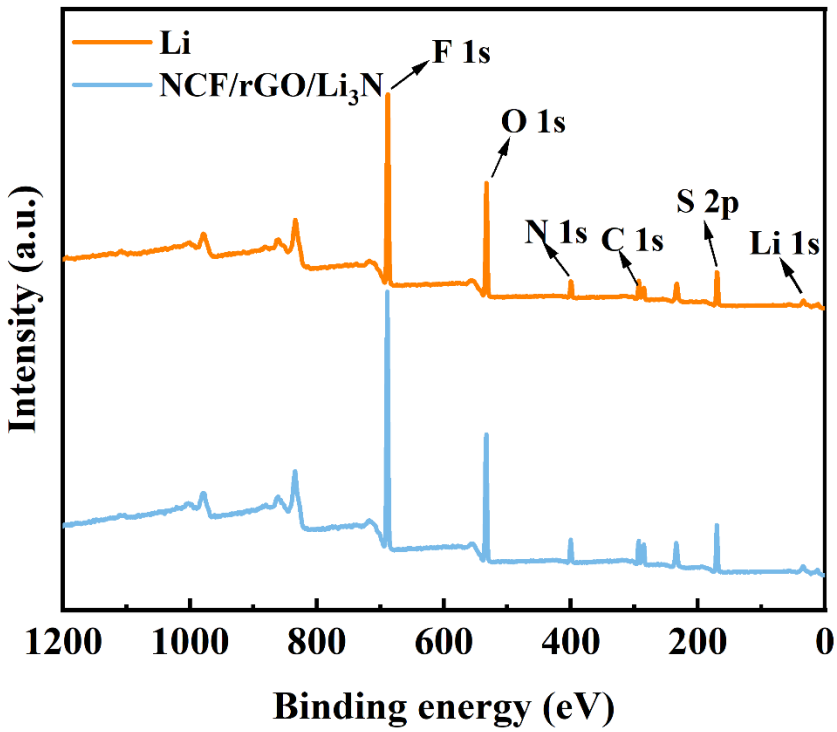

Fig. S23. The XPS survey spectrum of NCF/rGO/Li_3N and bare Li at 1 mA cm^{-2} and 0.5 mAh cm^{-2} after 100 cycles.

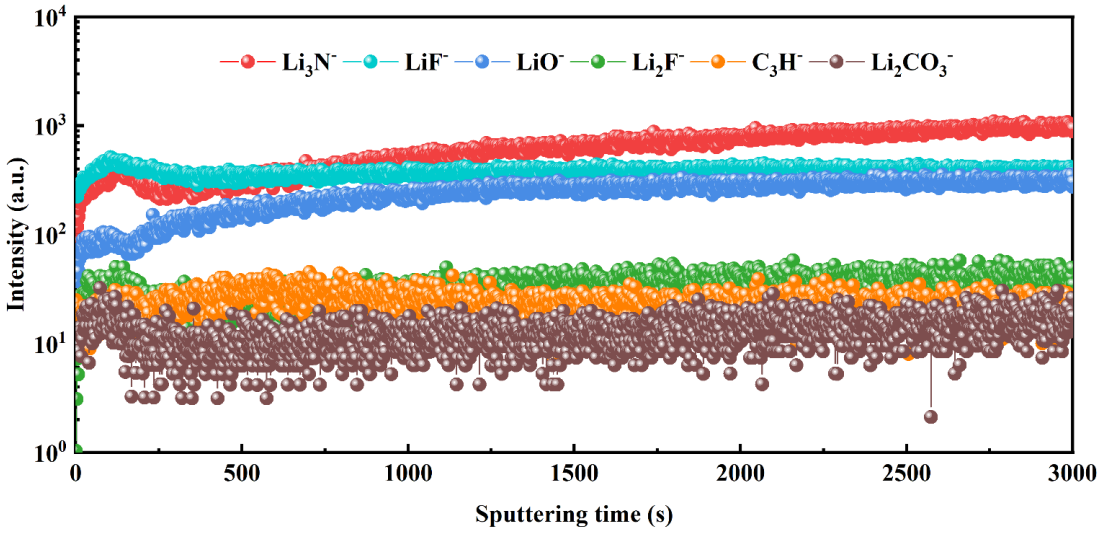

Fig. S24. TOF-SIMS depth profiles of NCF/rGO/Li_3N electrode after 100 Li plating/stripping cycles at 1 mA cm^{-2} and 0.5 mA h cm^{-2}.

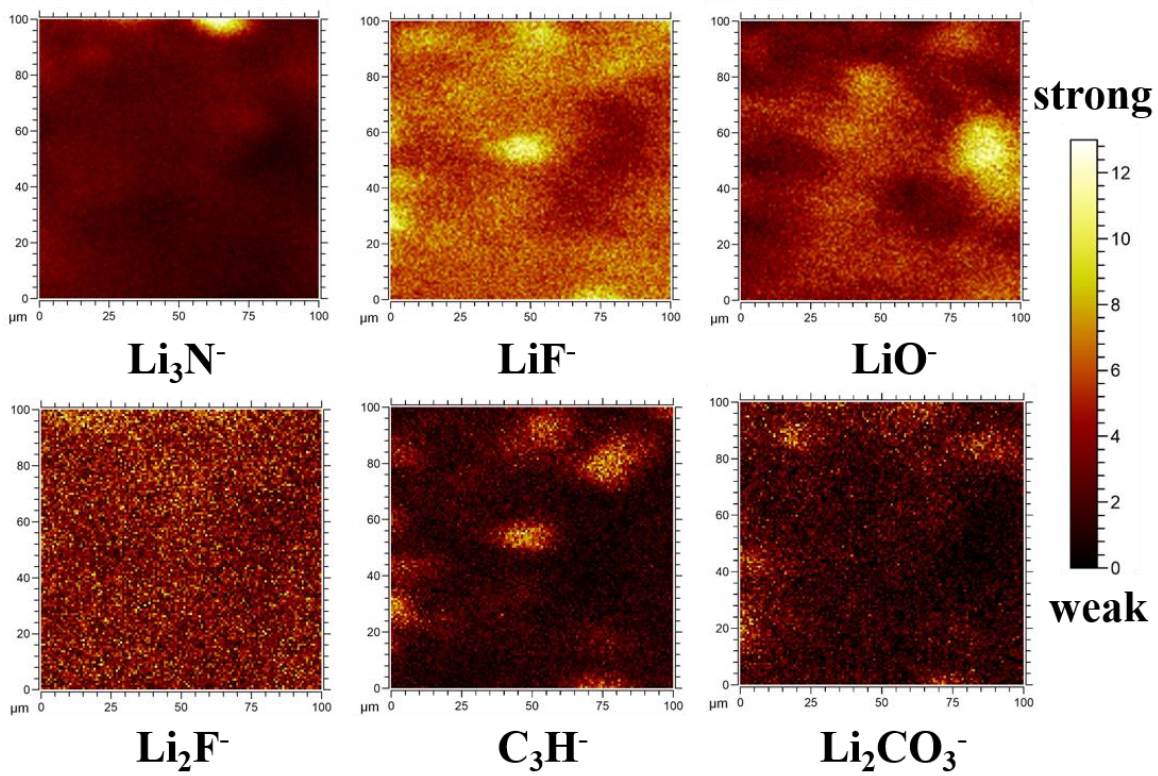

Fig. S25. Cross-profile images of TOF-SIMS depth sputtering in the surface of NCF/rGO/Li_3N electrode after 100 Li plating/stripping cycles at 1 mA cm^{-2} and 0.5 mA h cm^{-2}.

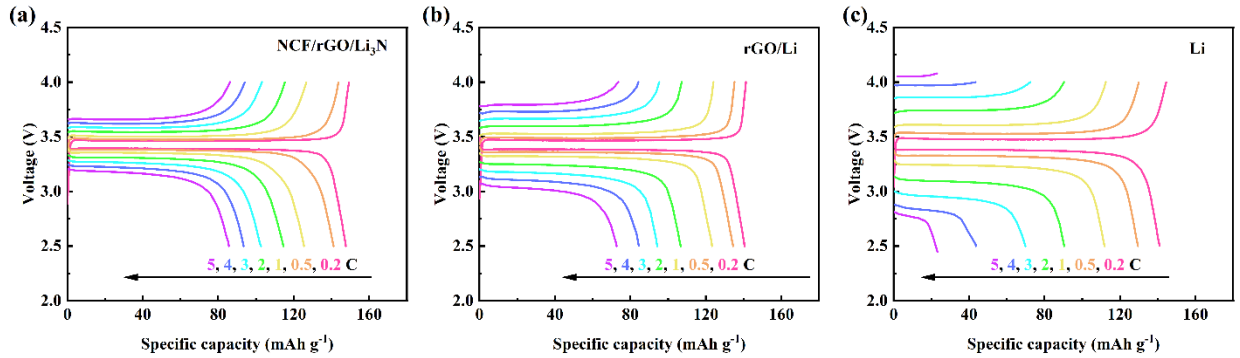

Fig. S26. Charge-discharge profiles of (a) NCF/rGO/Li_3N||LFP, (b) rGO/Li||LFP and (c) bare Li||LFP full cells at various rates.

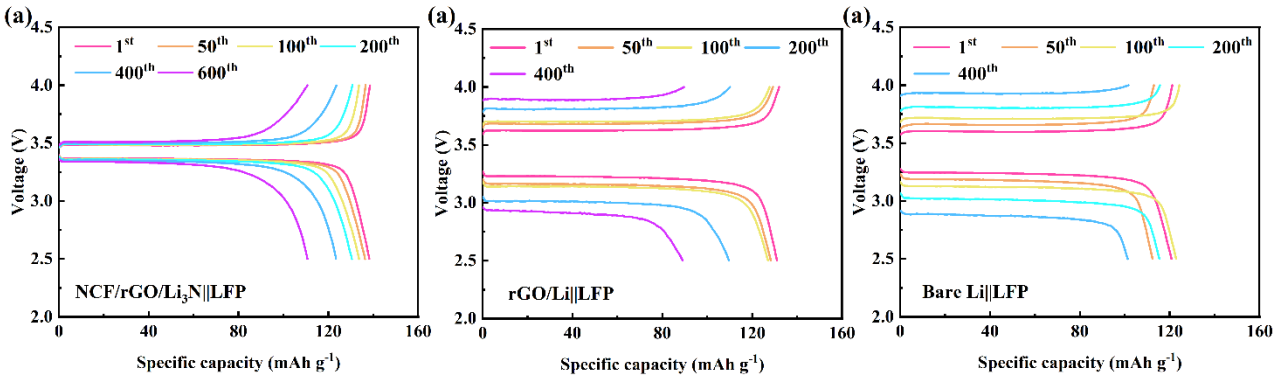

Fig. S27. Charge-discharge profiles of (a) NCF/rGO/Li_3N||LFP, (b) rGO/Li||LFP and (c) bare Li||LFP full cells at current density of 1C.

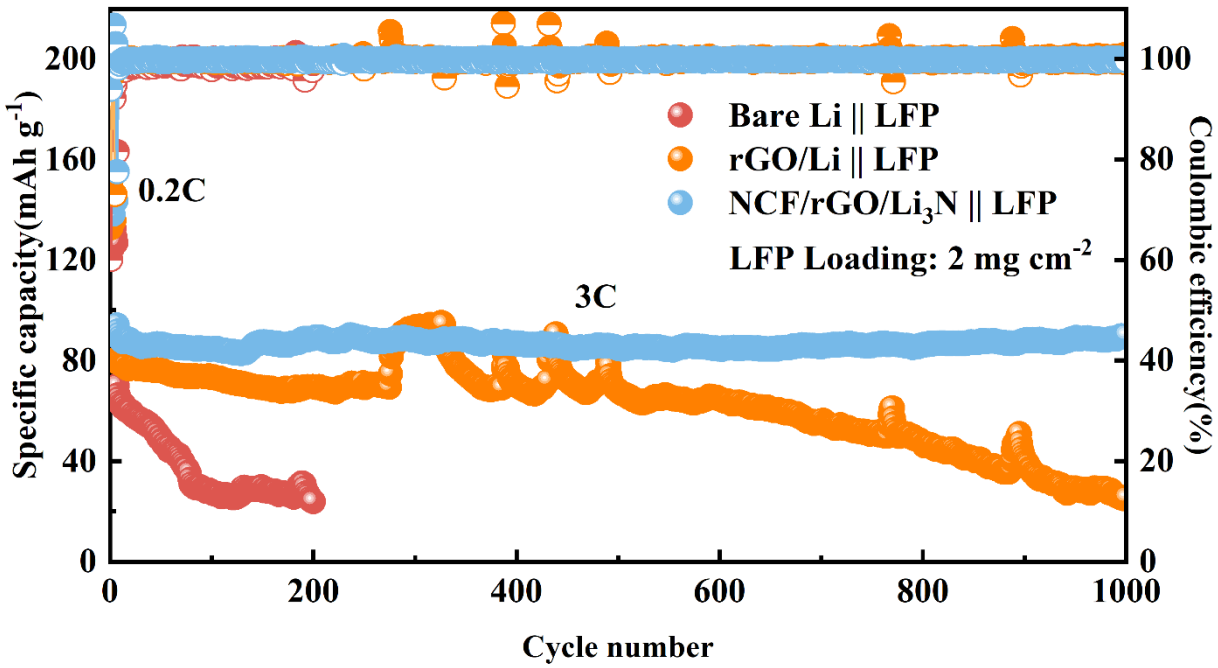

Fig. S28. Long-term cycling performance of NCF/rGO/Li_3N||LFP, rGO/Li||LFP and bare Li||LFP full cells at 3C (activate 5 cycles at 0.2C) (LFP loading is 2 mg cm^{-2}).

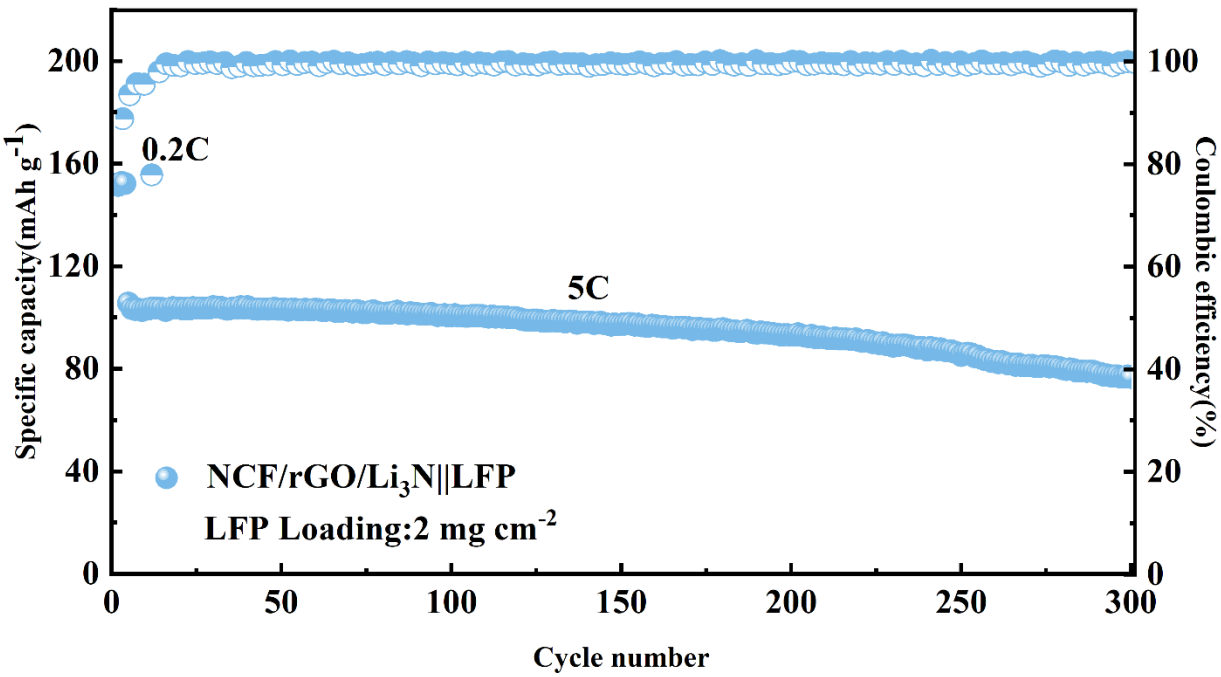

Fig. S29. Long-term cycling performance of NCF/rGO/Li_3N||LFP full cell at 5C (activate 5 cycles at 0.2C) (LFP loading is 2 mg cm^{-2}).

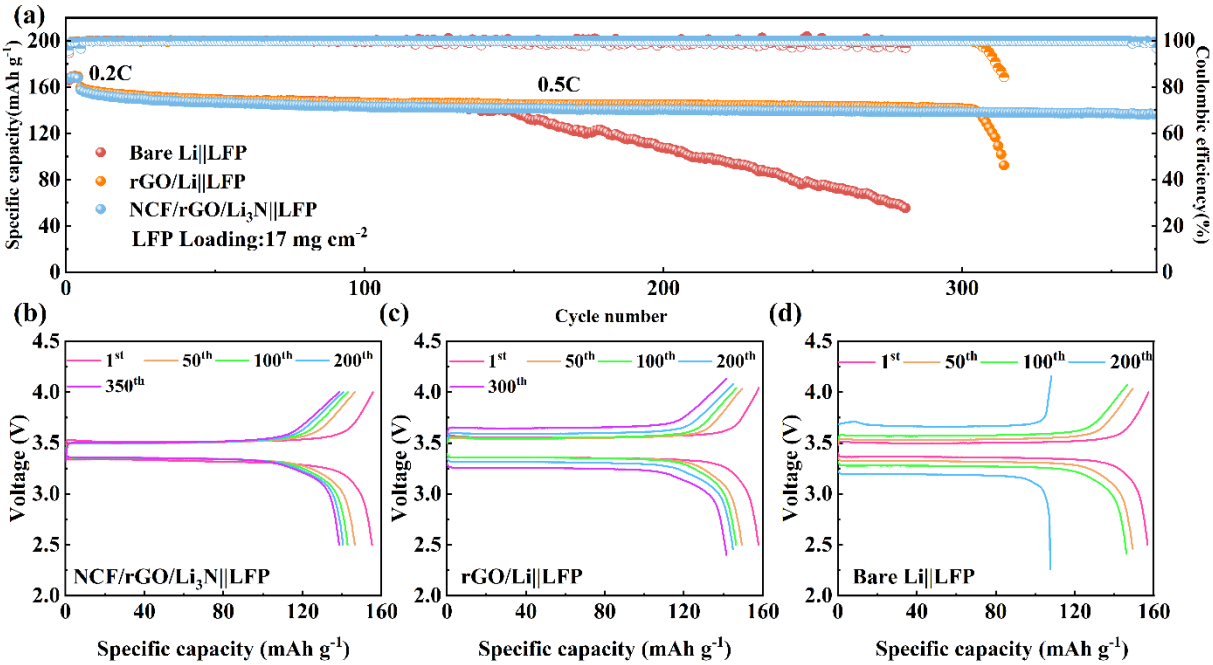

Fig. S30. Long-term cycling performance of NCF/rGO/Li_3N||LFP, rGO/Li||LFP and bare Li||LFP full cells at 0.5C (activate 5 cycles at 0.2C) (LFP loading is 17 mg cm^{-2}).

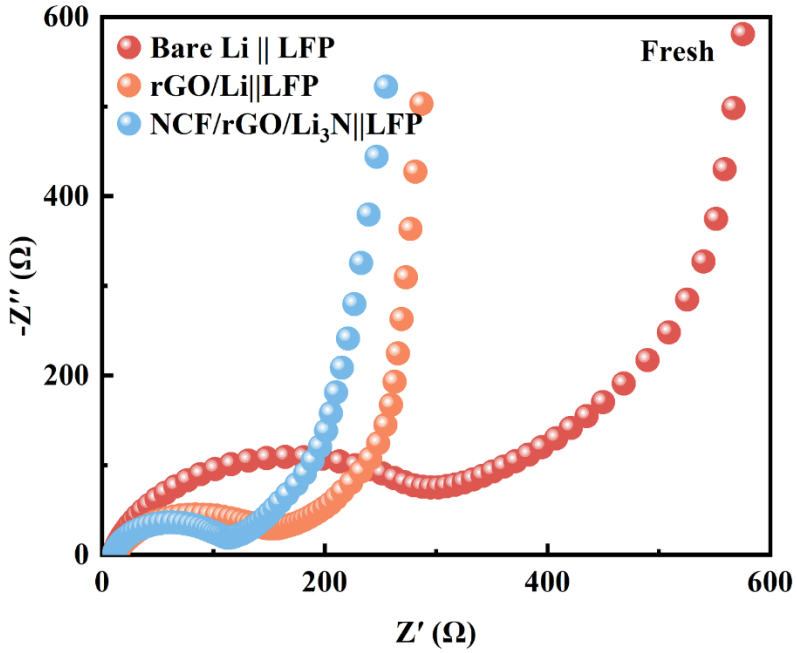

Fig. S31. EIS of NCF/rGO/Li_3N||LFP, rGO/Li||LFP, Bare Li||LFP full cell in fresh.

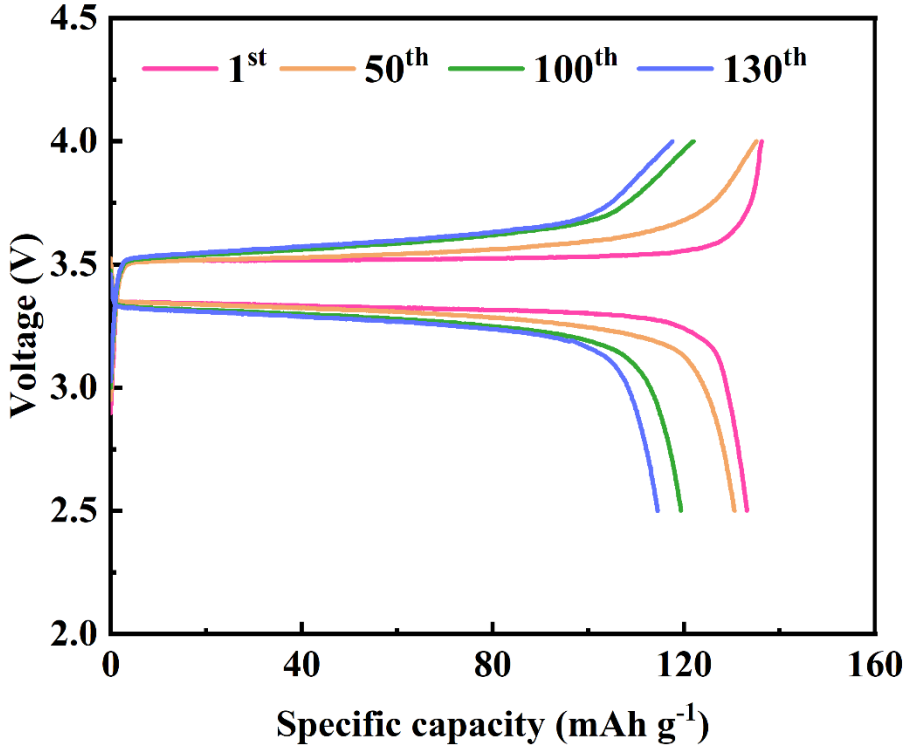

Fig. S32. Charge-discharge profiles of NCF/rGO/Li_3N||LLZO||LFP full cells at 0.1C.

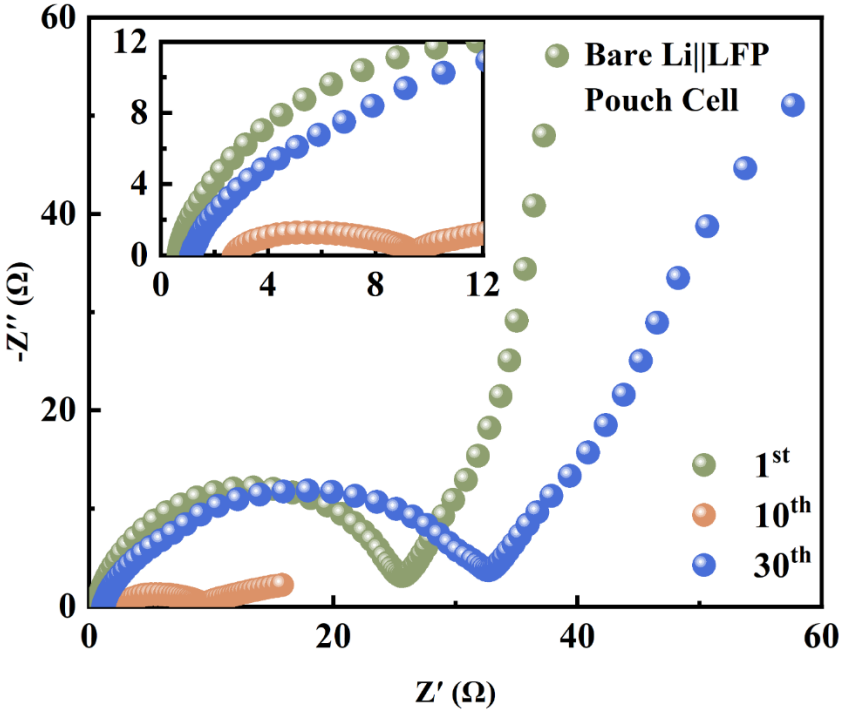

Fig. S33. Nyquist plots of bare Li||LFP pouch cell after 1 cycle,10 cycles and 30 cycles.

Table S1. Parameters of the NCF/rGO/Li_3N||NCM811 pouch cell.

Capacity	**181.6 mAh**
Cathode	**1.055 g**
Anode	**0.182 g**
Electrolyte	**0.89 g**
Separator	**0.12 g**
Mass	**2.247 g**